applied optics

Coplanar waveguide wideband band-stop filter based on localized spoof surface plasmons

Zhuo Li,* Jia Xu, Chen Chen, Yunhe Sun, Bingzheng Xu, Liangliang Liu, and Changqing Gu

Key Laboratory of Radar Imaging and Microwave Photonics, Ministry of Education, College of Electronic and Information Engineering, Nanjing University of Aeronautics and Astronautics, Nanjing 210016, China
**Corresponding author: lizhuo@nuaa.edu.cn*

Received 14 October 2016; revised 20 November 2016; accepted 20 November 2016; posted 23 November 2016 (Doc. ID 278579); published 15 December 2016

In this work, a wideband band-stop plasmonic filter based on localized spoof surface plasmons is reported, which consists of a coplanar waveguide (CPW) and an ultra-thin periodic corrugated metallic strip with defect units at the back of the substrate. Defect units are used to localize the transmission energy along the CPW. Each defect unit can introduce a narrow stop band, and a series of defect units is judiciously designed to form a broadband CPW band-stop filter. The center frequency and bandwidth of the filter can be tuned by the heights and numbers of the defect units. In addition, a *T*-shaped unit is designed to increase the equivalent height of the lateral branch so as to realize the miniaturization of the vertical geometric dimension. Theoretical analysis of the filter has been conducted, and a sample at microwave frequency has been fabricated and measured to validate our design. This simple band-stop plasmonic filter can find potential applications in plasmonic circuits and antennas at microwave and terahertz frequencies.

OCIS codes: (240.6680) Surface plasmons; (070.2615) Frequency filtering; (230.7390) Waveguides, planar.

https://doi.org/10.1364/AO.55.010323

1. INTRODUCTION

Surface plasmons (SPs), surface electromagnetic waves confined at the interface between metal and dielectric at optical frequencies, can overcome the diffraction limit due to strong subwavelength field confinement [1–3]. Surface plasmons have two existence forms as surface plasmon polaritons (SPPs) and localized surface plasmons (LSPs) [4,5]. Numerous studies on SPPs and LSPs have been conducted in the optical regime [6–10]. To overcome the PEC limit in the microwave and terahertz frequencies, spoof surface plasmon polaritons (SSPPs) that are supported by a metal surface with periodical one-dimensional grooves or two-dimensional holes have been proposed [11–13]. A series of SSPP devices has been designed, such as filters, waveguides, amplifiers, and frequency splitters [14–22]. In 2012, a pioneering study demonstrated that a periodically textured closed surface can support spoof LSPs at low frequencies [23]. Later on, multi-band spoof LSPs and spoof LSP modes in closed textured cavities were presented [24,25]. Compound spoof surface resonances and high-order spoof SPPs have also been demonstrated [26–29].

Recently, a simple band-notched coplanar waveguide (CPW) was reported, in which a defect unit or multiple defect units were introduced into the strip at the back of the CPW to generate a narrow stop band or multiple narrow stop bands [30]. This band-notched function is based on the idea that a defect mode exists in the band-gap between the fundamental mode and the first higher mode of the SSPPs [31]. The defect mode can be regarded as the localization of EM energy within the defect unit, which is different from previous studies in the localization mechanism [23–25]. In traditional spoof LSP structures, multiple resonances could be excited with each resonance peak being tuned coherently, resulting in rare applications of this kind of structure. However, in this scheme, the band-notch function can be easily introduced through appropriate coupling between the waveguide and the defects, and the center frequency and absorption level of the stop bands can be controlled by tuning the geometrical parameters of the defects with each stop band being adjusted independently.

Borrowing the idea from the previous works, we propose a broadband band-stop filter, which comprises a CPW and an ultra-thin corrugated metallic strip with a series of gradient defect branches at the back of the substrate. Three kinds of unit cells including *T*-shaped, *L*-shaped, and straight strips have been investigated. Compared with [30], *T*-shaped branches are introduced to avoid the over-length of the strip. Thus, the width of the strips at the upper layer could be designed small enough and the transition structure could be avoided [32]. In addition, a wide stop band can be realized by the introduction of several defects with gradient branch depths. To verify the performance of the proposed filter, we implemented experiments at microwave frequencies.

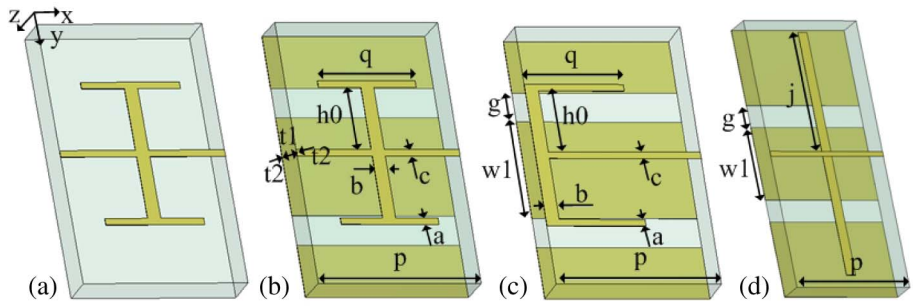

Fig. 1. Four different unit cells: $t1 = 1.0$ mm, $t2 = 0.018$ mm, $p = 5.0$ mm, $q = 3.0$ mm, $h0 = 1.9$ mm, $b = 0.4$ mm, $a = c = 0.2$ mm, and $j = h0 + q$. (a) Sketch of the T-shaped branch unit cell without the CPW layer. (b) Sketch of the T-shaped branch unit cell with the CPW layer. (c) Sketch of the L-shaped branch unit cell. (d) Sketch of the straight branch unit cell.

2. DISPERSION RELATION OF THE PLASMONIC WAVEGUIDE WITH DIFFERENT STRIPS

As shown in Fig. 1, four unit cells with different strips on the upper layer are presented, in which the specific dimensions are $p = 5.0$ mm, $q = 3.0$ mm, $h0 = 1.9$ mm, $b = 0.4$ mm, $a = c = 0.2$ mm, and $j = h0 + q$. The upper strips and the bottom CPW layers are set as PEC with the thickness $t2 = 0.018$ mm. The dielectric substrate is Rogers RT6010 (relative permittivity 10.2, loss tangent 0.0023) with the thickness $t1 = 1.0$ mm. The dimensions of the CPW in Figs. 1(b)–1(d) are designed with the width of the central conductor as 3 mm and the gap between the central conductor and ground as 0.9 mm. Unit cells shown in Figs. 1(a) and 1(b) are designed with and without the bottom metallic layer for comparison. As shown in Fig. 2(a), due to the strong coupling between the upper metal strip and bottom layer, the dispersion curve for the fundamental mode of the structure with the bottom layer significantly deviates from the light line, and its equivalent plasmonic frequency is much lower than that of the same structure without the bottom metallic layer. In addition, a band-gap between the fundamental and the first higher mode can be clearly observed.

The structure in Ref. [30] is designed based on a corrugated metallic saw tooth shape strip like that in Fig. 1(d), in which the width of the central conductor is too large and a transition structure is needed for the measurement. Figures 1(b) and 1(c) are two alternative modified models that can miniaturize the width of the SSPP strips when compared with the structure in Fig. 1(d). The dispersion relations of the three unit cells with the variations of q are calculated using the commercial software CST Microwave Studio. From the results in Figs. 2(b)–2(d) we can observe that the dispersion curves of the fundamental mode

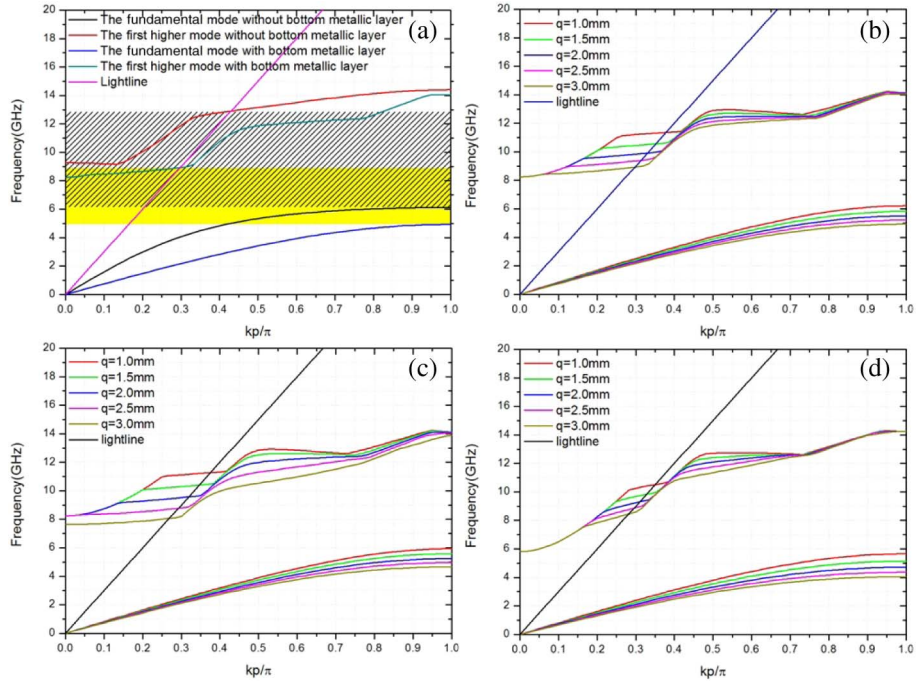

Fig. 2. (a) Dispersion curves of the T-shaped unit with and without bottom metallic layer. Yellow and shadowed areas represent the two band-gaps between the fundamental and the first higher mode of the two units. (b)–(d) Dispersion curves of the (b) T-shaped, (c) L-shaped, and (d) straight unit cells with the parameter q varying from 1.0 to 3.0 mm.

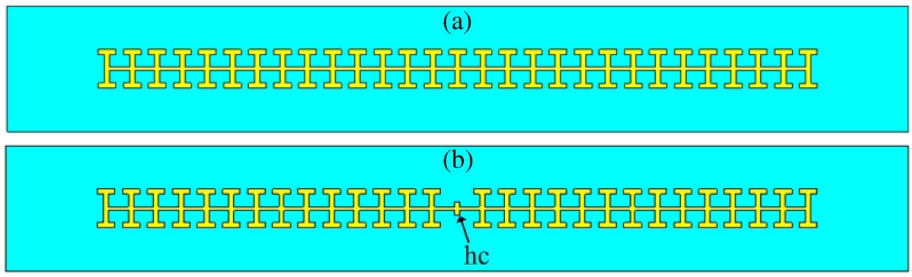

Fig. 3. (a) Schematic configuration of the waveguide with original metallic strip. (b) Schematic configuration of the waveguide with the metallic strip in which a defect is introduced and the height of the vertical branch is *hc*.

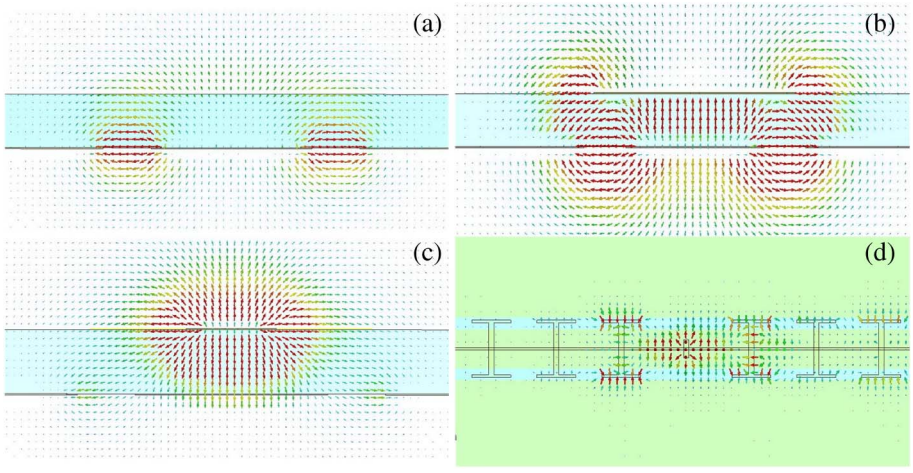

Fig. 4. (a) Electric-field distributions in the cross section of common CPW at 7.4 GHz. (b) Electric-field distributions in the cross section of the waveguide with the original strip in (a) at 7.4 GHz. (c) Cross section and (d) top view of electric-field distributions around the single defect at 5.8 GHz when hc = 1.0 mm.

and the first higher mode both vary with the variations of q from 1.0 to 3.0 mm. The larger the q, the lower the asymptotic frequency of the fundamental mode. In addition, the dispersion curves of the T-shaped and L-shaped unit cells are very similar. The method of miniaturization has already been reported in our previous paper [32] with small lateral geometric dimensioning. In this work, we also choose a T-shaped strip to design the filter.

3. STUDY OF THE WAVEGUIDE WITH THE ORIGINAL AND THE SINGLE-DEFECT STRIPS

Before we discuss the strip with defect units, we first investigate the transmission of the waveguide with the original strip [shown in Fig. 3(a)]. The upper layer, a periodic corrugated metallic strip, changes the field distributions of the transverse electromagnetic mode in the CPW. Without the strip, the electric fields are concentrated between the signal line and bilateral grounds as shown in Fig. 4(a). With the corrugated strip at the back of the substrate, energy can be coupled to the upper layer from the CPW as shown in Fig. 4(b), thus exciting SSPPs on the corrugated strip. Dispersion curves of the original unit [shown in Fig. 2(a)] clearly show that a band-gap exists between the fundamental mode and the first higher mode of the SSPPs structure. When a defect is introduced in Fig. 3(b), a localized mode is created at the defect. The electric fields are highly confined around the defect at a corresponding frequency in the

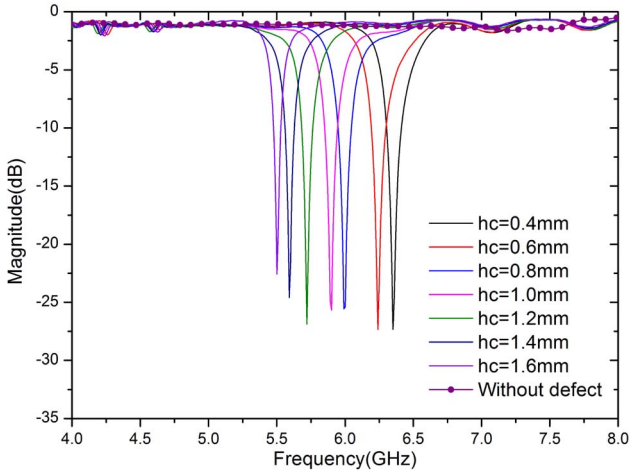

Fig. 5. Transmission spectra (S21) of the structure in Fig. 4(b) for various defect heights from 0.4 to 1.6 mm.

band-gap as shown in Figs. 4(c) and 4(d), forming a narrow stop band.

To study the characteristics of the defect mode, a series of hc has been chosen in Fig. 3(b). When hc changes from 0.4 to 1.6 mm with a step of 0.2 mm, a narrow-notched band appears and redshifts (the step is not the same as that shown in Fig. 5). The frequency independence of each notched band makes it possible to broaden the stop-band bandwidth by a series of defect branches with different depths.

4. BROADBAND PLAMONIC FILTER BASED ON LSSPs AND ITS EXPERIMENTAL VALIDATION AT MICROWAVE FREQUENCIES

Based on the defect mode, we have designed a compact and broadband band-stop CPW filter at microwave frequencies. As shown in Fig. 6, the proposed structure is designed on a 1-mm-thick substrate with permittivity 10.2 and loss tangent 0.0023. The overall size is 180 mm × 25 mm, and the thickness of the metal film is set as 0.018 mm. To achieve the

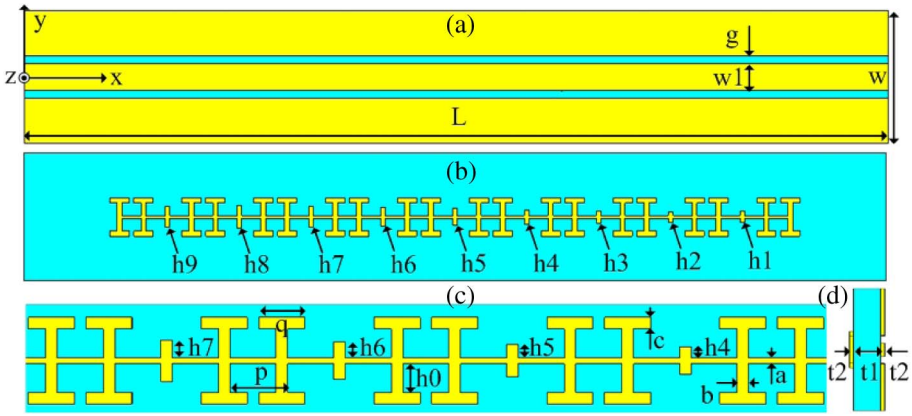

Fig. 6. Schematic configuration of the band-stop filter: (a) bottom view of the structure in which the detailed geometric data are $L = 180$ mm, $w = 25$ mm, $w1 = 3.0$ mm, and $g = 0.9$ mm. (b) Top view of the corrugated metallic strip with nine defects arranged every three periods in which the detailed geometric data are $h1 = 0.7$ mm, $h2 = 0.85$ mm, $h3 = 1.0$ mm, $h4 = 1.15$ mm, $h5 = 1.3$ mm, $h6 = 1.4$ mm, $h7 = 1.5$ mm, and $h8 = h9 = 1.6$ mm. (c) Enlarged schematic configuration of the strip in which $p = 5.0$ mm, $q = 3.0$ mm, $h0 = 1.9$ mm, $a = c = 0.2$ mm, and $b = 0.4$ mm. (d) Cross section of the dielectric substrate with the thickness $t1 = 1.0$ mm and $t2 = 0.018$ mm.

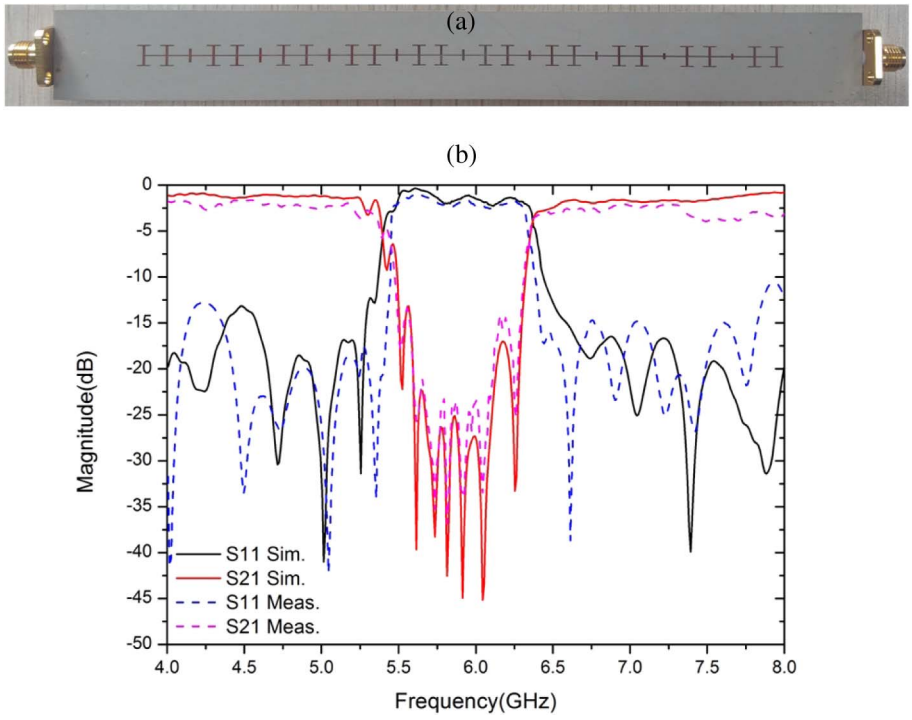

Fig. 7. (a) Sample with multi-defects strip at microwave frequencies. (b) Simulated (solid lines) and measured (dashed lines) results of the filter at microwave frequencies.

50 Ohm input impedance, the top layer is designed with the width of the central conductor being 3 mm and the gap between the central conductor and ground being 0.9 mm. A strip with defect units is introduced at the back of the substrate as shown in Fig. 6(c), in which nine defect branches are arranged every three periods. The dimensions of the original strip are $p = 5$ mm, $q = 3$ mm, $h0 = 2$ mm, $c = 0.2$ mm, $a = 0.2$ mm, and $b = 0.4$ mm, denoting the period of the original strip, the length of x-direction branches, the height of the y-direction branches, the width of x-direction branches, the width of the center line, and the width of the y-direction branches. The heights of the nine defect units are set as $h1 = 0.7$mm, $h2 = 0.85$ mm, $h3 = 1.0$ mm, $h4 = 1.15$ mm, $h5 = 1.3$ mm, $h6 = 1.4$ mm, $h7 = 1.5$ mm, $h8 = 1.6$ mm, and $h9 = 1.6$ mm, separately. The simulated reflection coefficients (S_{11}) and transmission coefficients (S_{21}) are given in Fig. 7(a). It is obvious that energy is confined around defect cells and the coupling between the upper and bottom layers guarantees the energy localization.

The key factor of the strip is that the width $w2 = a + 2 * (c + h0)$ should be assigned a suitable value. Due to the strong coupling between the SSPP waveguide and the CPW, the transmission efficiency outside the band-gap is reduced when $w2$ is larger than the width $w3 = w1 + 2 * g$. However, when $w2$ is smaller than $w3$, the coupling from the CPW to the SSPPs would become weak because less magnetic force of lines could cross the grooves, resulting in weak energy absorption around the defect in the band-gap. To guarantee the coupling outside the band-gap and ensure proper energy coupling in the band-gap, the width of the strip should be chosen appropriately. Thus, $w3 > w2 > w1$ has been selected as the rule in the design.

To verify the function of the compact broadband band-stop filter, we have fabricated a sample at microwave frequencies shown in Fig. 7(a). The S parameters have been measured with the help of the vector network analyzer (VNA, Agilent N5230C). The simulated and measured results are plotted in Fig. 7(b). We can observe that from 5.3 to 6.2 GHz S_{21} of the filter is lower than −15 dB and S_{21} is larger than −3 dB outside the stop band. Although there exists some discrepancy between the simulated and measured results due to the fabrication and material tolerance, the center frequency (5.8 GHz) and bandwidth (0.9 GHz) of the stop bands are in excellent agreement.

5. CONCLUSIONS

In summary, a wideband band-stop CPW filter based on localized spoof surface plasmons has been theoretically proposed and experimentally verified. Nine defect units are introduced in the periodic metallic strip at the back of the substrate, resulting in energy coupling from the CPW to the defect units that can form a wide stop band. This scheme can be used in a band-notched micro-strip line, slot line, and other planar transmission lines and can find potential applications in band-notched circuits and antenna design at microwave and terahertz frequencies.

Funding. Nanjing University of Aeronautics and Astronautics (NUAA) (SJLX150121, BCXJ15-04); Southeast University (SEU) (K201603); Natural Science Foundation of Jiangsu Province (BK20151480).

Acknowledgment. This work was supported in part by the Funding of the Jiangsu Innovation Program for Graduate Education, in part by the Foundation of the State Key Laboratory of Millimeter Waves, Southeast University, China, in part by the Funding for the Outstanding Doctoral Dissertation in NUAA, and in part by the Natural Science Foundation of Jiangsu Province and the priority academic program development of Jiangsu Higher Education Institutions.

REFERENCES

1. W. L. Barnes, A. Dereux, and T. W. Ebbesen, "Surface plasmon subwavelength optics," Nature **424**, 824–830 (2003).
2. D. K. Gramotnev and S. I. Bozhevolnyi, "Plasmonics beyond the diffraction limit," Nat. Photonics **4**, 83–91 (2010).
3. E. Ozbay, "Plasmonics: merging photonics and electronics at nanoscale dimensions," Science **311**, 189–193 (2006).
4. T. W. Ebbesen, C. Genet, and S. I. Bozhevolnyi, "Surface-plasmon circuitry," Phys. Today **61**(5), 44–50 (2008).
5. K. A. Willets and R. P. Van Duyne, "Localized surface plasmon resonance spectroscopy and sensing," Annu. Rev. Phys. Chem. **58**, 267–297 (2007).
6. N. Fang, H. Lee, C. Sun, and X. Zhang, "Sub diffraction-limited optical imaging with a silver superlens," Science **308**, 534–537 (2005).
7. M. Ozaki, J. Kato, and S. Kawata, "Surface-plasmon holography with white-light illumination," Science **332**, 218–220 (2011).
8. P. Muhlschlegel, H. J. Eisler, O. J. F. Martin, B. Hecht, and D. W. Pohl, "Resonant optical antennas," Science **308**, 1607–1609 (2005).
9. W. Li, P. H. C. Camargo, X. Lu, and Y. Xia, "Dimers of silver nanospheres: facile synthesis and their use as hot spots for surface-enhanced Raman scattering," Nano Lett. **9**, 485–490 (2009).
10. J. N. Anker, W. P. Hall, O. Lyandres, N. C. Shah, J. Zhao, and R. P. Van Duyne, "Biosensing with plasmonic nanosensors," Nat. Mater. **7**, 442–453 (2008).
11. F. J. Garcia-Vidal, L. Martin-Moreno, and J. B. Pendry, "Surfaces with holes in them: new plasmonic metamaterials," J. Opt. A **7**, S97–S101 (2005).
12. J. B. Pendry, L. Martin-Moreno, and F. J. Garcia-Vidal, "Mimicking surface plasmons with structured surfaces," Science **305**, 847–848 (2004).
13. A. P. Hibbins, B. R. Evans, and J. R. Sambles, "Experimental verification of designer surface plasmons," Science **308**, 670–672 (2005).
14. W. Zhu, A. Agrawal, and A. Nahata, "Planar plasmonic terahertz guided-wave devices," Opt. Express **16**, 6216–6226 (2008).
15. Q. Gan, Z. Fu, Y. J. Ding, and F. J. Bartoli, "Ultrawide-bandwidth slow-light system based on THz plasmonic graded metallic grating structures," Phys. Rev. Lett. **100**, 256803 (2008).
16. L. L. Liu, Z. Li, C. Q. Gu, B. Z. Xu, P. P. Ning, C. Chen, J. Yan, Z. Y. Niu, and Y. J. Zhao, "Smooth bridge between guided waves and spoof surface plasmon polaritons," Opt. Lett. **40**, 1810–1813 (2015).
17. L. L. Liu, Z. Li, B. Z. Xu, C. Q. Gu, C. Chen, P. P. Ning, J. Yan, and X. Y. Chen, "High-efficiency transition between rectangular waveguide and domino plasmonic waveguide," AIP Adv. **5**, 027105 (2015).
18. L. L. Liu, Z. Li, B. Z. Xu, P. P. Ning, C. Chen, J. Xu, X. L. Chen, and C. Q. Gu, "Dual-band trapping of spoof surface plasmon polaritons and negative group velocity realization through microstrip line with gradient holes," Appl. Phys. Lett. **107**, 201602 (2015).
19. A. I. Fernández-Domínguez, E. Moreno, L. Martin-Moreno, and F. J. Garcia-Vidal, "Terahertz wedge plasmon polaritons," Opt. Lett. **34**, 2063–2065 (2009).
20. D. Martín-Cano, M. L. Nesterov, A. I. Fernandez-Dominguez, F. J. Garcia-Vidal, L. Martin-Moreno, and E. Moreno, "Plasmons for subwavelength terahertz circuitry," Opt. Express **18**, 754–764 (2010).

21. W. Zhao, O. M. Eldaiki, R. Yang, and Z. Lu, "Deep subwavelength waveguiding and focusing based on designer surface plasmons," Opt. Express **18**, 21498–21503 (2010).
22. G. Kumar, S. Pandey, A. Cui, and A. Nahata, "Planar plasmonic terahertz waveguides based on periodically corrugated metal films," New J. Phys. **13**, 033024 (2011).
23. A. Pors, E. Moreno, L. Martin-Moreno, J. B. Pendry, and F. J. Garcia-Vidal, "Localized spoof plasmons arise while texturing closed surfaces," Phys. Rev. Lett. **108**, 223905 (2012).
24. Z. Li, L. L. Liu, C. Q. Gu, P. P. Ning, B. Z. Xu, Z. Y. Niu, and Y. J. Zhao, "Multi-band localized spoof plasmons with texturing closed surfaces," Appl. Phys. Lett. **104**, 101603 (2014).
25. Z. Li, B. Z. Xu, C. Q. Gu, P. P. Ning, L. L. Liu, Z. Y. Niu, and Y. J. Zhao, "Localized spoof plasmons in closed textured cavities," Appl. Phys. Lett. **104**, 251601 (2014).
26. Z. Liao, X. Shen, B. C. Pan, J. Zhao, Y. Luo, and T. J. Cui, "Combined system for efficient excitation and capture of LSP resonances and flexible control of SPP transmissions," ACS Photon. **2**, 738–743 (2015).
27. T. Jiang, L. Shen, X. Zhang, and L. X. Ran, "High-order modes of spoof surface plasmon polaritons on periodically corrugated metal surfaces," Prog. Electromagn. Res. M **8**, 91–102 (2009).
28. X. Zhang, L. Shen, and L. Ran, "Low-frequency surface plasmon polaritons propagating along a metal film with periodic cut-through slits in symmetric or asymmetric environments," J. Appl. Phys. **105**, 013704 (2009).
29. Z. Liao, Y. Luo, A. I. Fernández-Domínguez, X. Shen, S. A. Maier, and T. J. Cui, "High-order localized spoof surface plasmon resonances and experimental verifications," Sci. Rep. **5**, 9590 (2015).
30. B. Z. Xu, Z. Li, L. L. Liu, J. Xu, C. Chen, P. P. Ning, X. L. Chen, and C. Q. Gu, "Tunable band-notched coplanar waveguide based on localized spoof surface plasmons," Opt. Lett. **40**, 4683–4686 (2015).
31. S. H. Kim, S. S. Oh, K. J. Kim, J. E. Kim, H. Y. Park, O. Hess, and C. S. Kee, "Subwavelength localization and toroidal dipole moment of spoof surface plasmon polaritons," Phys. Rev. B **91**, 035116 (2015).
32. J. Xu, Z. Li, L. L. Liu, C. Chen, B. Z. Xu, P. P. Ning, and C. Q. Gu, "Low-pass plasmonic filter and its miniaturization based on spoof surface plasmon polaritons," Opt. Commun. **372**, 155–159 (2016).